g-Engineering in Hybrid Rotaxanes to Create AB and AB_2 Electron Spin Systems: EPR Studies of Weak Interactions Between Dissimilar Electron Spin Qubits

Antonio Fernandez,[†] *Eufemio Moreno Pineda,*[†,§] *Christopher A. Muryn,*[†] *Stephen Sproules,*[†,‡] *Fabrizio Moro,*[†,¥] *Grigore A. Timco,*[†] *Eric J. L. McInnes,*[†] *and Richard E. P. Winpenny*[†,*]

[†]School of Chemistry and Photon Science Institute, The University of Manchester, Oxford Rd, Manchester M13 9PL, United Kingdom.

[§]Present address: Institute of Nanotechnology, Karlsruhe Institute of Technology, D-76344 Eggenstein-Leopoldshafen, Germany.

[‡]Present address: WestCHEM, School of Chemistry, University of Glasgow, Glasgow G12 8QQ, United Kingdom.

[¥]Present address: School of Physics and Astronomy, The University of Nottingham, University Park, Nottingham NG7 2RD, United Kingdom.

E-mail: richard.winpenny@manchester.ac.uk

Keywords: EPR spectroscopy; heterometallic complexes; magnetic properties; quantum computing; rotaxane

Abstract. Hybrid [2]rotaxanes and pseudo-rotaxanes are reported where the magnetic interaction between dissimilar spins is controlled to create AB and AB_2 electron spin systems, allowing independent control of weakly interacting $S = {}^1/_2$ centers

Several groups have proposed the idea that molecules could be used as electron spin qubits.[1-6] Molecular qubits can be designed such that phase memory times (T_m) approach other solid state electron spin technologies,[7] and have the advantage of being functionalizable by synthetic chemistry methods. Proposed molecular spin qubits include organic radicals,[2] simple coordination complexes,[7] high-spin[1] and low-spin clusters,[3-5] and 4f ions.[6] One challenge is to bring together ensembles of such qubits, and particularly to bring together qubits with different electronic *g*-factors, so called *g*-engineering,[2,6] which would allow the qubits to be addressed individually and controllably within a complex molecule. Takui and co-workers have done this using elegant organic chemistry, and have reported the operation of the CNOT gate using such an approach.[2] Here we show how similar *g*-engineering can be achieved using coordination chemistry of 3d-metal cages.

We have been studying heterometallic $\{Cr_7M\}$ rings for their fascinating spin physics.[8] Where M is Ni, antiferromagnetic exchange coupling gives a well-isolated $S = {}^1/_2$ ground state; pulsed EPR spectroscopy shows these have sufficiently long phase memory times to use as qubits.[9] The chemical robustness and versatility of these units allow their incorporation in hybrid [2]rotaxanes.[10] Here we use a thread, $PyCH_2NHCH_2CH_2Ph$, that features a pyridyl group as a stopper on one end, and a benzyl group as stopper at the other end, and make the [2]rotaxane $[PyCH_2NH_2CH_2CH_2Ph][Cr_7Ni(\mu\text{-}F)_8(O_2C^tBu)_{16}]$ **1** in 32% yield (see Supporting Information).

Stoichiometric reaction of **1** with [Cu(hfac)$_2$] (Hhfac = 1,1,1,6,6,6-hexafluoroacetylacetonate) yields a further [2]rotaxane {[Cu(hfac)$_2$][PyCH$_2$NH$_2$CH$_2$CH$_2$Ph][Cr$_7$Ni(μ-F)$_8$(O$_2$C^{t}Bu)$_{16}$]} **2**; X-ray crystallography[11] confirms that [Cu(hfac)$_2$] has bound to the pyridyl of the rotaxane-thread (Figure 1a,b and Figure S1 in the Supporting Information). The heterometallic ring is unchanged from the rotaxane **1**, containing eight metals in an octagon, bridged by fluoride and pivalates (Figure 1b). The ammonium group of the thread H-bonds to the fluorides within the metal octagon. The pyridyl group from the thread binds to copper, occupying the apical site of a square-based pyramid. The distance between the centroid of the {Cr$_7$Ni} ring and the Cu(II) is 7.332(1) Å, while the average Cu···Cr/Ni distance is 8.56 Å with the Cr···Cu vectors making an average angle ¸ of 31° to the {Cr$_7$Ni} normal (which is parallel to the Cu–N vector, Figure 1c).

The only through-bond pathway between the spin centers of the {Cr$_7$Ni} ring and the single Cu(II) site, involves hydrogen-bonds between fluorides and the protonated ammonium site of the thread, therefore any magnetic interactions between the two components is expected to be very weak. Nevertheless, clear evidence of such interactions is observed by continuous wave (cw) EPR spectroscopy (Figure 2).

At low temperature (5 K) only the S = $^1/_2$ ground state of {Cr$_7$Ni} is populated substantially; this state is approximately axially symmetric with $g_{\perp}^{Cr7Ni}$ H 1.78, $g_{||}^{Cr7Ni}$ H 1.74 where the “unique” axis is perpendicular to the {Cr$_7$Ni} plane.[12] The EPR spectrum of **2** at Q-band (34 GHz) and 5 K is very simple with two sets of features, centered at the g-values expected for {Cr$_7$Ni} and for Cu ($g_{\perp}^{Cu}$ H 2.05, $g_{||}^{Cu}$ H 2.30) with resolution of copper hyperfine (A^{Cu}) on $g_{||}^{Cu}$. Each of these g-features is split into a spectroscopic doublet; i.e. the spectrum has the form of a simple AB spin pattern, where the spin-spin coupling is much smaller than the difference in Zeeman energy (the latter is 0.17 cm^{-1} for

a static field of 1.21 T and g = 2.1 and 1.8). This is a picture familiar from NMR spectroscopy, but examples of AB electron spin patterns resolved by cw EPR are rare.[2a,13]

The resolution is such that we can read the parallel and perpendicular components of the interaction (J) between the Cu and {Cr_7Ni} sites directly from the spectrum. Because the local z-axis at the Cu site (along the Cu–N vector) is parallel to the normal of the {Cr_7Ni} ring, the $g_{||}^{Cu}$ and $g_{||}^{Cr7Ni}$ axes correspond to the same molecular orientation of **2**. The multiplet pattern on $g_{||}^{Cu}$ clearly shows two overlapping hyperfine quartets (^{63,65}Cu, $I = {}^3/_2$), hence $J_{||}$ is of the same order as $A_{||}^{Cu}$. Measurement of the doublet splittings of the $g_\perp$ features then reveals that $J_\perp \approx J_{||}$, i.e. the interaction is essentially isotropic. To test this we simulated[14] the spectrum with a simple isotropic exchange Hamiltonian:

$$\hat{H} = \mu_B \hat{S}_{Cu} \cdot \mathbf{g}_{Cu} \cdot \vec{B} + \mu_B \hat{S}_{Cr7Ni} \cdot \mathbf{g}_{Cr7Ni} \cdot \vec{B} + \hat{S}_{Cu} \cdot \mathbf{A}_{Cu} \cdot \hat{I}_{Cu} - J \hat{S}_{Cu} \cdot \hat{S}_{Cr7Ni}.$$

We initially fixed the g-values and Cu hyperfine interaction from model complexes, with J as the only free variable, but then refined all parameters: better fits are found by introducing a slight rhombicity in g (Figure 2a). This gives J = –0.032 cm^{-1}; the relative transition intensities within the exchange doublets are sensitive to the sign of J.

The interaction is weak and anti-ferromagnetic, but it is perhaps surprising it is seen at all as the only through-bond pathway involves H-bonds. As the interaction is isotropic this implies that it cannot be dipolar (through-space) in origin. For comparison, we have calculated the dipolar interaction for **2**. A very crude treatment is to take {Cr_7Ni} as a spin localised at its centroid: this gives $D_{xx,yy}$ = +0.004, D_{zz} = –0.009 cm^{-1}. This is too weak to explain the spectrum and moreover such a model cannot, by definition, give an isotropic interaction. A more rigorous treatment is to calculate the full dipolar interaction matrix **D** for the nine-spin system: the effective {Cr_7Ni}···Cu interaction can be calculated by the sum of the individual Cr···Cu and Ni···Cu dipolar interactions weighted

by the projection factors of the Cr and Ni local spins onto the $S = {}^1/_2$ ground state of the {Cr_7Ni} ring (see the Supporting Information).[16] We used spin projection factors determined from solid-state ^{53}Cr NMR studies on $(Me_2NH_2)[Cr_7NiF_8(O_2C^tBu)_{16}]$.[17] The full calculated dipolar matrix is in the SI: the leading term (along $g_{||}$) is D_{zz} = –0.0034 cm^{-1} i.e. an order of magnitude smaller than the experimentally observed coupling, and including this **D** matrix makes no significant difference to the calculated EPR spectrum. Hence, the ring···Cu couplings are not due to dipolar interactions. The pathway for the isotropic exchange interaction remains unclear but must be through bond. Interestingly, the value found here falls within the range predicted by Coffman and Buettner's[15] empirical limit function for long-range superexchange interactions. In the cases they discuss there are always more obvious through bond pathways.

This result led us to explore closely related but more complex hetero-spin systems. Firstly, $[Cu(NO_3)_2(Me_2CO)]\{[PyCH_2NH_2CH_2CH_2Et][Cr_7NiF_8(O_2C^tBu)_{16}]\}_2$ **3** was synthesized, which contains two *pseudo*-[2]rotaxanes bound to a single Cu(II) site (Figure 3a). The thread in **3** differs from that in **1** and **2**, with an ethyl-group at one end rather than a benzyl; this could in principle allow dethreading in solution but this is not observed as proved by the form of its EPR spectrum. The Cu site has the two pyridyls from the *pseudo*-rotaxanes *trans* to each other, with two nitrates and an acetone coordinated in the plane. The nitrates are chelating with one long (2.6 Å) and one short (1.95 Å) Cu–O distance each. The two Cu–N and the two short Cu–O(nitrate) distances define a square plane (N–Cu–N and O–Cu–O 168 and 175°, respectively) with the acetone in an axial position (Cu–O 2.41 Å). Hence the best description of the Cu geometry seems to be again square pyramidal, but now with the axial orientation perpendicular to the {Cr_7Ni} planes.

Secondly, to increase the complexity further, a [3]rotaxane was made about an axle with a pyridyl at each end: $[\{PyCH_2NH_2(CH_2)_5\}_2][Cr_7NiF_8(O_2C^tBu)_{16}]_2]$ **4**.[18] Coordination

of a [Cu(hfac)$_2$] unit to each end of **4** then gives: [Cu(hfac)$_2$(H$_2$O)]$_2$[{PyCH$_2$NH$_2$(CH$_2$)$_5$}$_2$][Cr$_7$NiF$_8$(O$_2$C^{t}Bu)$_{16}$]$_2$] **5** (Figure 3b). The copper coordination geometry is now six-coordinate with two hfac ligands and a water; the latter is *cis* to the pyridyl. The Cu–O/N distances are surprisingly regular (Cu–N 2.21; Cu–O 2.126–2.162 Å). Hence it is unclear where the "unique" Cu axis is. The relationship between the {Cr$_7$Ni} rings and Cu ions in both **3** and **5** are similar to that in **2**, because in each case the ring is formed around the ammonium site of R-NH$_2$CH$_2$CH$_2$-py where the pyridyl binds to the Cu [**3**: {Cr$_7$Ni} centroid···Cu 7.34 and 7.07 Å; average Cr···Cu 8.44 Å; average ¸ 31°; **5**: {Cr$_7$Ni} centroid···Cu 7.34 Å; average Cr···Cu 8.54 Å; average ¸ 31°].

For both **3** and **5** the Q-band EPR spectra of frozen solutions at 5 K again show weak coupling. For **3** an AB$_2$ spin system pattern is obtained, with the resonance due to the {Cr$_7$Ni} ring (the "B" spin) split into a doublet, while the Cu resonances (the "A" spin) are split into 1:2:1 triplets (Figure 2b). The spectrum of **4** is very similar to that of **1**, i.e. that of an isolated {Cr$_7$Ni} ring, where any ring···ring interaction within the [3]rotaxane is very weak and not observable by cw EPR. The spectrum of **5** is very similar to that of **2** with a weak {Cr$_7$Ni}···Cu interaction; the spin structure (as regards cw EPR) is therefore two very weakly or non-interacting AB spin pairs (Figure 2c). Simulations of **3** and **5** both give J = –0.020 cm^{-1} (Figure 2). Although the relationship between the {Cr$_7$Ni} and Cu fragments are similar in each case, minor changes in the spin coupling are justified because of the differing coordination geometry at Cu. In **2** the "unique" (z) axis of the Cu ion (defining the orientation of the $d_{x^2-y^2}$ magnetic orbital) is unambiguously parallel to the {Cr$_7$Ni}···Cu axis (or equivalently the Cu–N direction). In **3**, this axis is orthogonal to {Cr$_7$Ni}···Cu; the situation in **5** is ambiguous.

The weak coupling regime of AB spin systems allows the spins to be addressed individually. This is the basis of Takui and co-workers' "*g*-engineering" approach to

construct a CNOT gate with dissimilar organic radicals,[2] and towards Lloyd's proposal of periodic $(ABC)_n$ arrays using inequivalently orientated metal ions in helicates.[19] The hetero-spin structure of **2**, and its dimerization into a more complex array in **5**, shows how such arrays can be achieved exploiting the facile coupling between molecules enabled by coordination and supramolecular chemistry approaches.

An important question is whether such complex systems can be constructed without deleterious effects on the spin coherence properties of the components. To test this we measured the phase memory times (T_m) for **2** and **5** by pulsed EPR at X-band using a standard Hahn echo sequence [$\pi/2 - \tau - \pi - \tau - echo$]. Static magnetic field positions were chosen that selectively pumped EPR transitions on the {Cr_7Ni} ring and on the Cu site (409 and 310 mT, respectively, for **2**; Figure S4 in the Supporting Information). T_m for the {Cr_7Ni} component is ca. 600 ns at 5 K in both **2** and **5** (Figure S5 in the Supporting Information). This is in the 400-700 ns range (depending on R) found for isolated $[R_2NH_2][Cr_7NiF_8(O_2C^tBu)_{16}]$ at 5 K.[9] T_m times for the Cu resonance are larger, at 1.0 μs for both **2** and **5**, and of the same order as found for related isolated Cu(II) complexes, e.g. [Cu(hfac)$_2$(4,4-Me$_2$-bipy)] has 3 μs at 5 K.[20] Hence, the phase memory times are not significantly reduced due to the inter-spin interaction. This bodes well for performing spin manipulation experiments in supramolecular arrays of molecular nanomagnets.

The next steps require tuning the interaction strengths and Zeeman frequencies such that the components can be addressed individually within the resonator bandwidths available with current pulsed microwave technology. The interaction strength will be controllable through supramolecular chemistry. The difference in Zeeman frequency could be achieved, e.g. with spin clusters of marginally different g[21] or with homo-spin clusters exploiting non-parallel orientations and g-anisotropy.[22]

Acknowledgments. This work was supported by the EPSRC(UK, EP/L018470/1), the National EPR Facility and the European Commission (Marie Curie Intra-European Fellowship to AF (300402)). EMP thanks the Panamanian agency SENACYT-IFARHU for funding. We also thank EPSRC (UK) for funding an X-ray diffractometer (grant number EP/K039547/1).

Suplementary Information. Supporting information for this article is available on the WWW under http://dx.doi.org/10.1002/anie.201504487.

References

[1] M. Leuenberger, D. Loss, *Nature* **2001**, *410*, 789.

[2] a) S. Nakazawa, S. Nishida, T. Ise, T. Yoshino, N. R. Mori, D. Rahimi, K. Sato, Y. Morita, K. Toyota, D. Shiomi, M. Kitagawa, H. Hara, P. Carl, P. Hçfer, T. Takui, *Angew. Chem. Int. Ed.* **2012**, *51*, 9860; *Angew. Chem.* **2012**, *124*, 9998; b) K. Sato, S. Nakazawa, R. Rahimi, T. Ise, S. Nishida, T. Yoshino, N. Mori, K. Toyota, D. Shiomi, Y. Yakiyama, Y. Morita, M. Kitagawa, K. Nakasuji, M. Nakahara, H. Hara, P. Carl, P. Hçfer, T. Takui, *J. Mater. Chem.* **2009**, *19*, 3739.

[3] F. Meier, J. Levy, D. Loss, *Phys. Rev. Lett.* **2003**, *90*, 47901.

[4] F. Troiani, A. Ghirri, M. Affronte, S. Carretta, P. Santini, G. Amoretti, S. Piligkos, G. Timco, R. E. P. Winpenny, *Phys. Rev. Lett.* **2005**, *94*, 207208.

[5] J. Lehmann, A. Gaita-AriÇo, E. Coronado, D. Loss, *Nat. Nanotechnol.* **2007**, *2*, 312.

[6] D. Aguilà, L. A. Barrios, V. Velasco, O. Roubeau, A. Repollés, P. J. Alonso, J. Sesé, S. J. Teat, F. Luis, G. Aromì, *J. Am. Chem. Soc.* **2014**, *136*, 14215.

[7] a) K. Bader, D. Dengler, S. Lenz, B. Endeward, S.-D. Jiang, P. Neugebauer, J. v. Slageren, *Nat. Commun.* **2014**, *5*, DOI: 10.1038/ncomms6304; b) M. Warner, S. Din, I. S. Tupitsyn, G. W. Morley, A. Stoneham, J. A. Gardener, Z. Wu, A. J. Fisher, S. Heutz, C. W. M. Kay, G. Aeppli, *Nature* **2013**, *503*, 504; c) M. J. Graham, J. M. Zadrozny, M. Shiddiq, J. S. Anderson, M. S. Fataftah, S. Hill, D. E. Freedman, *J. Am. Chem. Soc.* **2014**, *136*, 7623.

[8] a) M. Affronte, S. Carretta, G. A. Timco, R. E. P. Winpenny, *Chem. Commun.* **2007**, 1789; b) G. A. Timco, E. J. L. McInnes, R. E. P. Winpenny, *Chem. Soc. Rev.* **2013**, *42*, 1796.

[9] a) A. Ardavan, O. Rival, J. J. L. Morton, S. J. Blundell, A. M. Tyryshkin, G. A. Timco, R. E. P.Winpenny, *Phys. Rev. Lett.* **2007**, *98*, 057201; b) C. J. Wedge, R. E. George, G. A. Timco, F. Tuna, S. Rigby, E. J. L. McInnes, R. E. P. Winpenny, S. J. Blundell, A. Ardavan, *Phys. Rev. Lett.* **2012**, *108*, 107204.

[10] a) C.-F. Lee, D. A. Leigh, R. G. Pritchard, D. Schultz, S. J. Teat, G. A. Timco, R. E. P. Winpenny, Nature 2009, 458, 314; b) B. Ballesteros, T. B. Faust, C.-F. Lee, D. A. Leigh, C. A. Muryn, R. G. Pritchard, D. Schultz, S. J. Teat, G. A. Timco, R. E. P. Winpenny, *J. Am. Chem. Soc.* **2010**, *132*, 15435.

[11] a) Crystal data for **2** [$C_{104}H_{163}Cr_7CuF_{20}N_2O_{36}Ni$]: M_r = 2883.61, orthorhombic, space group *Pnaa*, T = 100.15 K, a = 20.2386(7), b = 27.6927(6), c = 27.4034(9) Å, V=15358.6(8) Å^3, Z = 4, $Á$ = 1.247 g cm^{-3}, total data = 13572, R_1 = 0.1238 for I e 2$Ã(I)$ and wR_2 = 0.3326. Crystal data for **3** [$C_{179}H_{320}Cr_{14}CuF_{16}N_6Ni_2O_{71}$]: M_r = 4905.35, orthorhombic, space group *Pna*2$_1$, T = 150.15 K, a = 51.6574(10), b = 27.1191(6), c = 20.0038(3) Å, V = 28023.4(9) Å^3, Z = 4, $Á$ = 1.163 g cm^{-3}, total data = 36449, R_1 = 0.0993 for I e 2$Ã(I)$ and wR_2 = 0.2468. CCDC 1401242 (**2**), 1401243 (**3**), and 916469 (**5**) contain the supplementary crystallographic data for this paper. These data can be

obtained free of charge from The Cambridge Crystallographic Data Centre. Crystallographic data for **2** was collected on a Bruker Prospector CCD diffractometer with CuK± radiation (» = 1.5418 Å). Crystallographic data for **3** was collected on an Agilent SuperNova CCD diffractometer with MoK± radiation (» = 0.71073 Å) and was solved using SHELX; b) G. M. Sheldrick, *Acta Crystallogr. Sect. A* **2008**, *64*, 112.

[12] S. Piligkos, H. Weihe, E. Bill, F. Neese, H. El Mkami, G. M. Smith, D. Collison, G. Rajaraman, G. A. Timco, R. E. P. Winpenny, E. J. L. McInnes, *Chem. Eur. J.* **2009**, *15*, 3152.

[13] G. R. Eaton, S. S. Eaton, *Acc. Chem. Res.* **1998**, *31*, 107.

[14] Using EasySpin: S. Stoll, A. Schweiger, *J. Magn. Reson.* **2006**, *178*, 42.

[15] R. E. Coffman, G. R. Buettner, *J. Phys. Chem.* **1979**, *83*, 2387.

[16] C. Elsässer, M. Brecht, R. Bittl, *J. Am. Chem. Soc.* **2002**, *124*, 12606.

[17] C. M. Casadei, L. Bordonali, Y. Furukawa, F. Borsa, E. Garlatti, A. Lascialfari, S. Carretta, S. Sanna, G. Timco, R. E. P. Winpenny, *J. Phys. Condens. Matter* **2012**, *24*, 406002.

[18] G. F. S. Whitehead, B. Cross, L. Carthy, V. A. Milway, H. Rath, A. Fernandez, S. L. Heath, C. A. Muryn, R. G. Pritchard, S. J. Teat, G. A. Timco, R. E. P. Winpenny, *Chem. Commun.* **2013**, *49*, 7195.

[19] a) S. Lloyd, *Science* **1993**, *261*, 1569; b) Y. Morita, Y. Yakiyama, S. Nakazawa, T. Murata, T. Ise, D. Hashizume, D. Shiomi, K. Sato, M. Kitagawa, K. Nakasuji, T. Takui, *J. Am. Chem. Soc.* **2010**, *132*, 6944.

[20] J. M. Burchfield, J.-L. Du, K. M. More, S. S. Eaton, G. R. Eaton, *Inorg. Chim. Acta* **1997**, *263*, 23.

[21] G. A. Timco, E. J. L. McInnes, R. G. Pritchard, F. Tuna, R. E. P. Winpenny, *Angew. Chem. Int. Ed.* **2008**, *47*, 9681; *Angew. Chem.* **2008**, *120*, 9827.

[22] T. B. Faust, V. Bellini, A. Candini, S. Carretta, L. Carthy, D. Collison, R. J. Docherty, J. Kenyon, G. Lorusso, J. Machin, E. J. L. McInnes, C. A. Muryn, R. G. Pritchard, S. J. Teat, G. A. Timco, F. Tuna, G. F. S. Whitehead, W. Wernsdorfer, M. Affronte, R. E. P. Winpenny, *Chem. Eur. J.* **2011**, *17*, 14020.

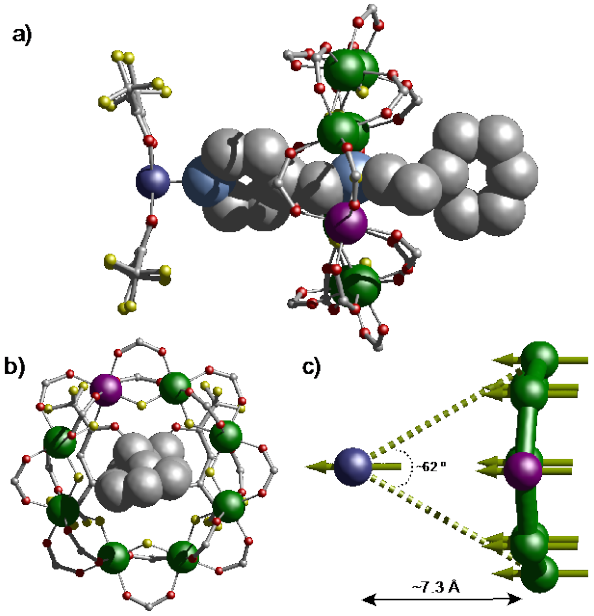

Figure 1. Crystal structure of **2** (ball and stick) viewed (a) side-on, and (b) perpendicular to the {Cr_7Ni} plane; (c) Arrow representation of the g_z-component of the Cu(II) and {Cr_7Ni}. The dotted lines are Cu···M vectors for opposite M sites on the {Cr_7Ni} ring, the average "trans" M–Cu–M angle is shown. Atom colours: Cr, green; Ni, purple; Cu, indigo; F, yellow; O, red; C, grey; N, pale blue. H-atoms and ^{t}Bu groups of pivalates omitted for clarity. C and N atoms of thread larger to highlight this structural feature.

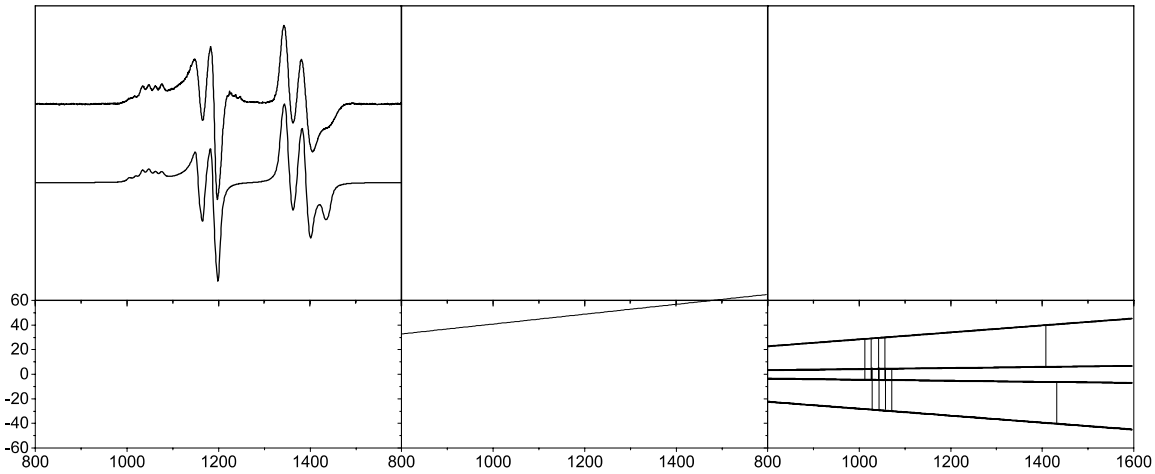

Figure 2. Experimental Q-band (ca. 34 GHz) EPR spectra (black) and simulations (red) for (a) **2**, (b) **3**, and (c) **5** in 1:1 toluene:CH_2Cl_2 solution at 5 K. Simulation parameters: (a) $g_{x,y,z}^{Cr7Ni}$= 1.780, 1.765, 1.710; $g_{x,y,z}^{Cu}$ = 2.065, 2.045, 2.325; A_z^{Cu} = 450 MHz; J = –0.032 cm^{-1}; (b) $g_{x,y,z}^{Cr7Ni}$ = 1.785, 1.775, 1.715; $g_{x,y,z}^{Cu}$ = 2.050, 2.020, 2.287; A_z^{Cu} = 450 MHz; J = –0.020 cm^{-1}; and (c) $g_{x,y,z}^{Cr7Ni}$ = 1.780, 1.775, 1.705; $g_{x,y,z}^{Cu}$ = 2.060, 2.045, 2.322; A_z^{Cu} = 450 MHz; J = –0.020 cm^{-1}. (d-f) Zeeman plots for H along the molecular z axis, with Q-band EPR transitions shown.

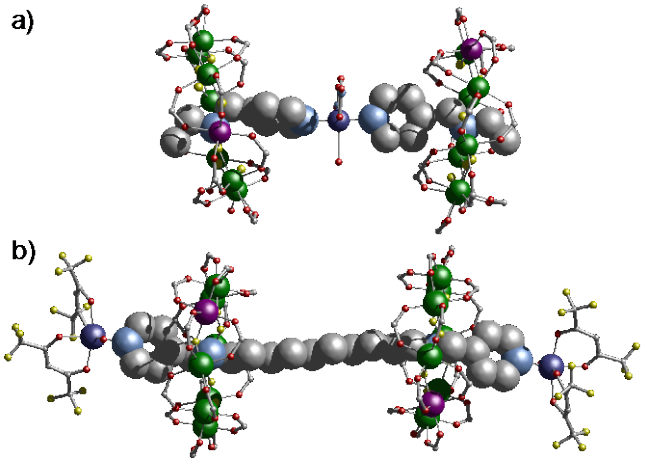

Figure 3. Side view crystal structure (ball and stick) of (a) *pseudo*-[2]rotaxanes **3** and (b) [3]rotaxane **5**. Atom colours: Cr, green; Ni, purple; Cu, indigo; F, yellow; O, red; C, grey; N, pale blue. H-atoms and ^{t}Bu groups of pivalates omitted for clarity.

Supporting Information

g-Engineering in Hybrid Rotaxanes to Create AB and AB_2 Electron Spin Systems: EPR Studies of Weak Interactions Between Dissimilar Electron Spin Qubits

Antonio Fernandez,[†] *Eufemio Moreno Pineda,*[†,§] *Christopher A. Muryn,*[†] *Stephen Sproules,*[†,‡] *Fabrizio Moro,*[†,¥] *Grigore A. Timco,*[†] *Eric J. L. McInnes,*[†] *and Richard E. P. Winpenny*[†,*]

[†]School of Chemistry and Photon Science Institute, The University of Manchester, Oxford Rd, Manchester M13 9PL, United Kingdom.

[§]Present address: Institute of Nanotechnology, Karlsruhe Institute of Technology, D-76344 Eggenstein-Leopoldshafen, Germany.

[‡]Present address: WestCHEM, School of Chemistry, University of Glasgow, Glasgow G12 8QQ, United Kingdom.

[¥]Present address: School of Physics and Astronomy, The University of Nottingham, University Park, Nottingham NG7 2RD, United Kingdom.

Experimental Details

Unless stated otherwise, all reagents and solvents were used without further purification. The syntheses of the hybrid organic-inorganic rotaxanes were carried out in Erlenmeyer Teflon® FEP flasks supplied by Fisher. Column chromatography was carried out using Silica 60A (particle size 35-70 μm, Fisher, UK) as the stationary phase, and TLC was performed on precoated silica gel plates (0.25 mm thick, 60 F254, Merck, Germany) and observed under UV light. NMR spectra were recorded on Bruker AV 400, and Bruker DMX 500 instruments. Chemical shifts are reported in parts per million (ppm) from low to high frequency and referenced to the residual solvent resonance. ESI mass spectrometry and microanalysis were carried out by the services at The University of Manchester. Compounds **3** and **5** were prepared according to reference *Chem. Commun.* **2013**, *49*, 7195-7197.

Synthetic methods

1. Synthesis of *N*-benzyl-2-phenylethanamine (*L*)

Systematic name: To a solution of 4-pyridine carboxaldehyde (1.68 g, 16.5 mmol) in 30 mL of methanol, phenethylamine (2.08 mL, 16.5 mmol) in 5 mL methanol was added and the reaction mixture was refluxed for 3 h under nitrogen atmosphere, allowed to stir at room temperature overnight. $NaBH_4$ (5 equiv) was added and reaction mixture was stirred during 12 h under nitrogen atmosphere. The reaction was quenched with water and the solvent was evaporated. The solid was extracted with chloroform, washed with water and dried over anhydrous magnesium sulfate and evaporated. A light yellow liquid was obtained in 68% yield (2.2 g). ESI-MS (sample dissolved in MeOH, run in MeOH): *m*/*z* = 213 $[M+H]^+$. ^1H NMR (400 MHz, 293 K, $CDCl_3$): ´ = 2.81-2.93 (m, 4H), 3.75 (s, 2H), 7.00-7.3 (m 7H), 8.4 (d, 2H).

2. Synthesis of Rotaxane (1)

*[2]rotaxane (**1**)*: Pivalic acid (20.0 g, 195 mmol), *L* (0.6 g, 2.4 mmol), and $CrF_3 \cdot 4H2O$ (3.0 g, 16 mmol) were heated at 140 °C with stirring in a Teflon flask for 30 min, then $[Ni_2(\mu\text{-}H_2O)(O_2C^tBu)_4(HO_2C^tBu)_4]$ (0.35 g, 0.6 mmol) was added. After 1 h the temperature of the reaction was increased to 160 °C for 20 h. The flask was cooled to room temperature, acetonitrile (35 mL) was added while stirring and a green microcrystalline precipitated was collected by filtration, washed with a large quantity of acetonitrile and dried in air. Flash chromatography (toluene, then gradient elution up to 9:1 toluene/EtOAc) afforded desired

[2]-rotaxane as a green crystalline solid. Yield: 1.9 g (32%). Elemental analysis (%) calcd for $C_{94}H_{161}Cr_7F_8N_2NiO_{32}$: Cr 15.12, Ni 2.43, C 46.92, H 6.74, N 1.16: found: Cr 15.07, Ni 2.35, C 46.90, H 7.02, N 1.17. ESI-MS (sample dissolved in THF, run in MeOH): *m*/*z* = 2427 $[M+Na]^+$; 2405$[M+H]^+$.

3. Synthesis of Rotaxane (2)

*Rotaxane dimer (**2**)*: $[Cu(hfacac)_2]$ (0.06 g, 0.12mmol) was added to a solution of **1** (0.3 g, 0.12mmol) in acetone (25 mL), and the mixture was heated and stirred until the copper complex dissolved. The crystalline product was filtered, washed with acetone and dried in air. Yield: 0.09 g (52%; yield based on Cu). Elemental analysis (%) calcd for **2**: Ni $C_{104}H_{165}Cr_7F_{20}N_2NiO_{36}Cu$: Cr 12.61, Ni 2.03,Cu 2.20, C 43.28, H 5.76, N 0.97; found: Cr 12.70, Ni 2.04, Cu 2.07, C 42.68, H 5.56, N 0.97.

4. Synthesis of pseudorotaxane (3)

The precursor $[PyCH_2NH_2Et][Cr_7Ni(\mu\text{-}F)_8(O_2C^tBu)_{16}]$ was prepared by the method given in *Angew. Chem. Int. Ed.* **2005**, *44*, 6496-6500.

*Pseusdorotaxane (**3**):* To a warm solution of $[PyCH_2NH_2Et][Cr_7Ni(\mu\text{-}F)_8(O_2C^tBu)_{16}]$ (0.9 g, 0.386 mmol) in acetone (120 mL) was added $Cu(NO_3)_2{\cdot}3H_2O$ (0.03 g, 0.124 mmol) and the solution was briefly stirred, then it was filtered and the filtrate was left undisturbed in a sealed flask at room temperature. Dark green crystals (including some suitable for X-ray structure study) slowly formed over five days. Crystals were filtered off and washed with acetone. Yield: 0.51 g (84%) (based on Cu). Elemental analysis (%): calc. for $C_{179}H_{320}Cr_{14}CuF_{16}N_6Ni_2O_{71}$: Cr 14.84, Ni 2.39, Cu 1.30, C 43.83, H 6.58, N 1.71; found: Cr 14.57, Ni 2.35, Cu 1.22, C 43.99, H 5.95, N 1.62.

Crystallography

The data of **2** was recorded on a Bruker Prospector CCD diffractometer with CuK± radiation (» = 1.5418 Å). The structure was solved by direct methods and refined against F^2 using SHELXTL. CCDC 1401242, 1401243 and 916469 contains the supplementary crystallographic data for this paper. These data can be obtained free of charge via www.ccdc.cam.ac.uk/conts/retrieving.html (or from the Cambridge Crystallographic Data Centre, 12 Union Road, Cambridge CB21EZ, UK; fax: (+44)1223-336-033; or deposit@ccdc.cam.ac.uk).

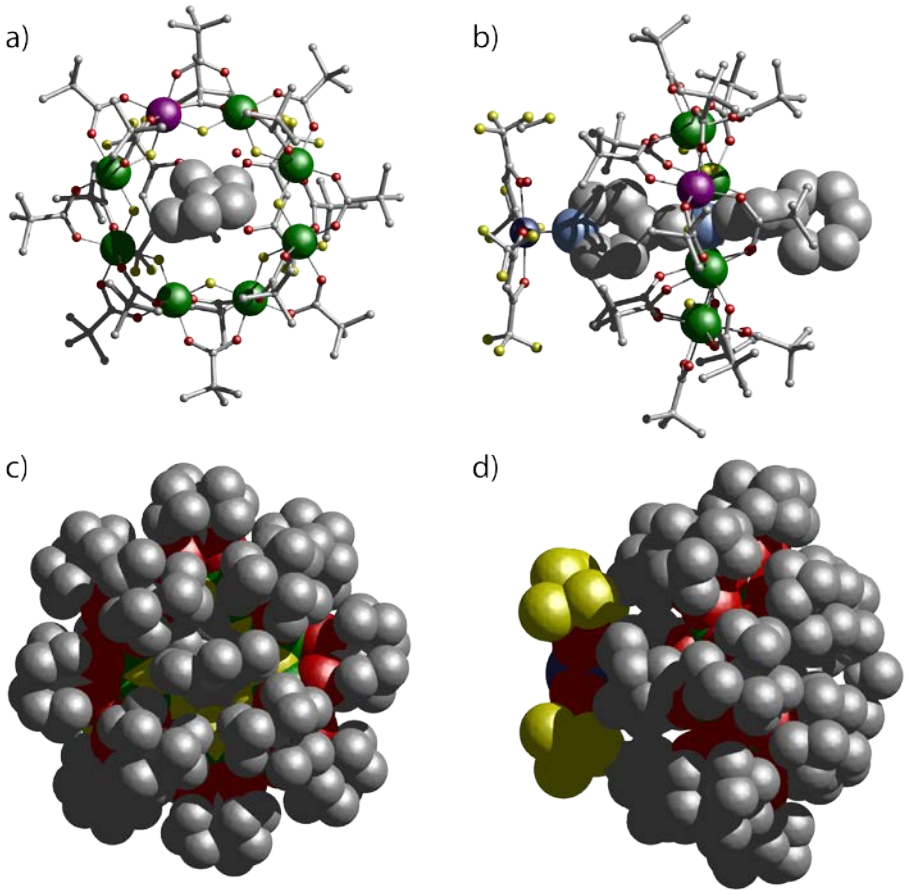

Figure S1. Crystal structure of **2** (ball and stick) (a) along the C_2 axis and (b) side view of the {Cr_7Ni} H-atoms omitted for clarity. Space filling representation (c) along the C_2 axis and (d) side view of the {Cr_7Ni}. Colours: Cr, green; Ni, purple; Cu, indigo; F, yellow; O, red; C, grey; N, pale blue; H, dark grey.

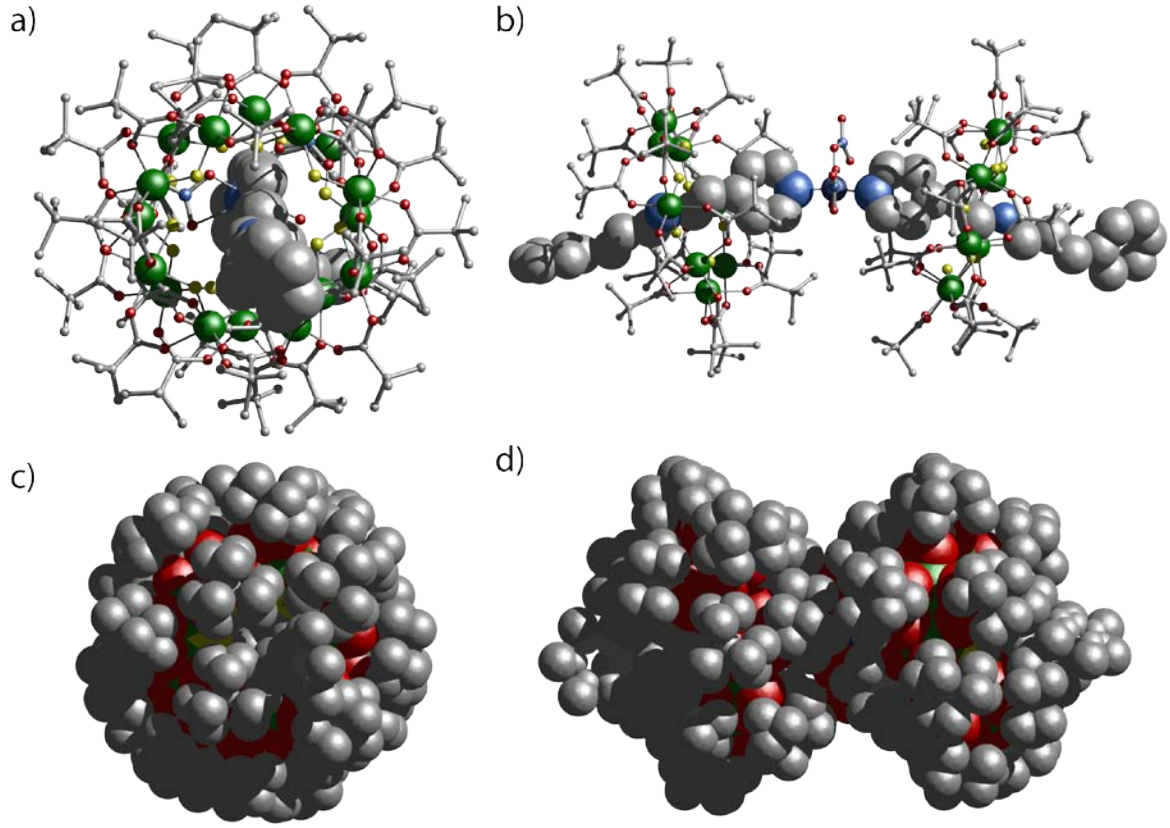

Figure S2. Crystal structure of **3** (ball and stick) (a) along the C_2 axis and (b) side view of the {Cr_7Ni} H-atoms omitted for clarity. Space filling representation (c) along the C_2 axis and (d) side view of the {Cr_7Ni}. Colours: Cr, green; Ni, purple; Cu, indigo; F, yellow; O, red; C, grey; N, pale blue; H, dark grey.

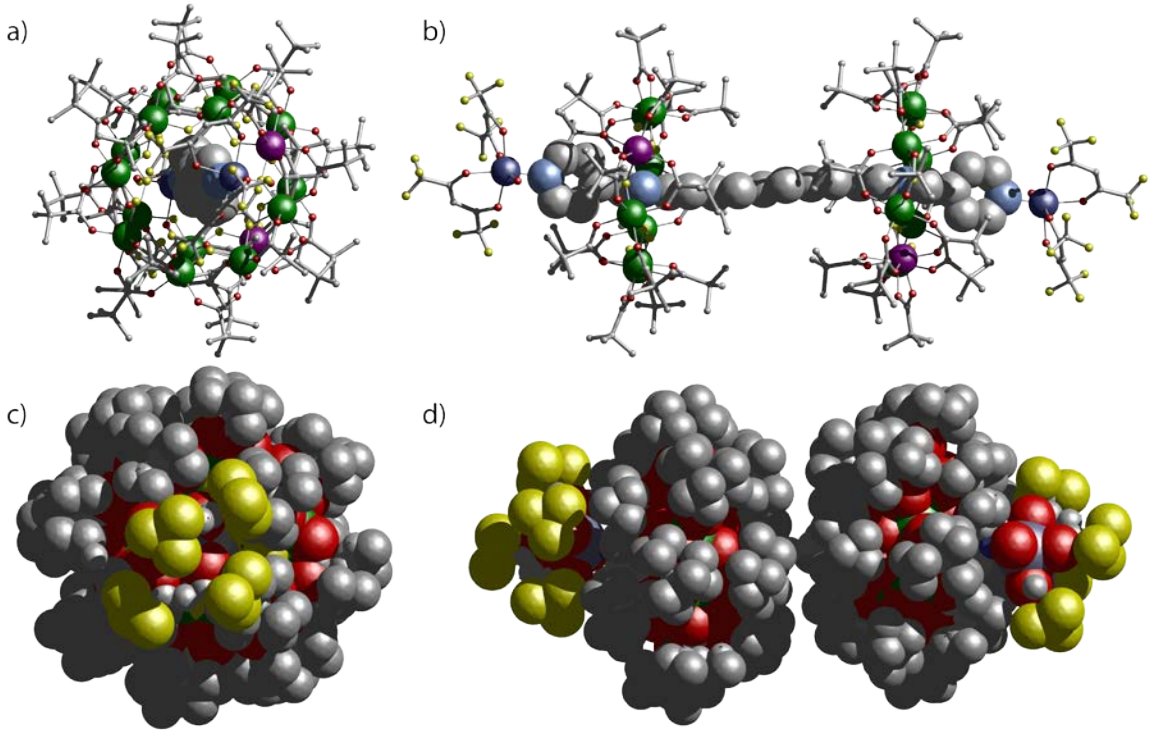

Figure S3. Crystal structure of **5** (ball and stick) (a) along the C_2 axis and (b) side view of the {Cr_7Ni}. H-atoms omitted for clarity. Space filling representation (c) along the C_2 axis and (d) side view of the {Cr_7Ni}. Colours: Cr, green; Ni, purple; Cu, indigo; F, yellow; O, red; C, grey; N, pale blue H, dark grey.

EPR measurements

X-band (~9.5 GHz) and Q-band (~34 GHz) EPR spectra were recorded with a Bruker ELEXSYS E580 FT EPR spectrometer. The data were collected on polycrystalline powders and toluene/dichloromethane (1:1) solutions at 5 K. Spectral simulations were performed using the EasySpin 4.5.5 simulation software.[14]

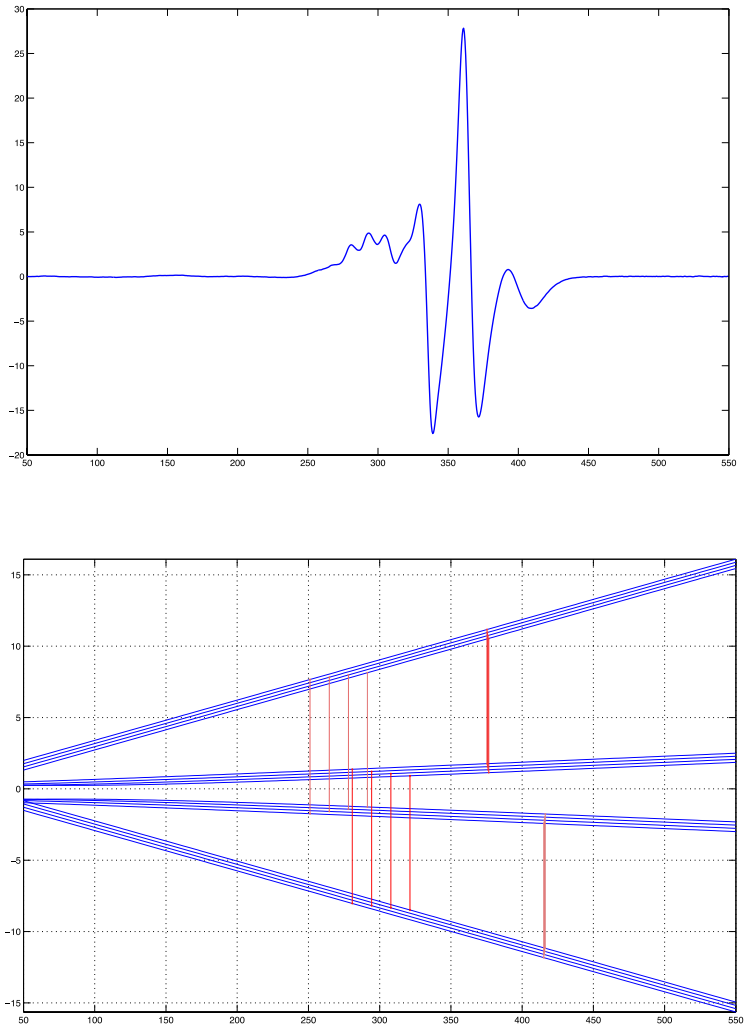

Figure S4. Top: X-band (9.405 GHz) EPR spectrum of compound **2** in 1:1 toluene/CH_2Cl_2 solution at 5 K. Bottom: Zeeman diagram for magnetic field parallel to the molecular *z* axis with X-band transitions shown in red. For the pulsed EPR measurements in Figure S5, the static magnetic fields were 314 and 409 mT, associated with Cu and {Cr_7Ni} transitions, respectively.

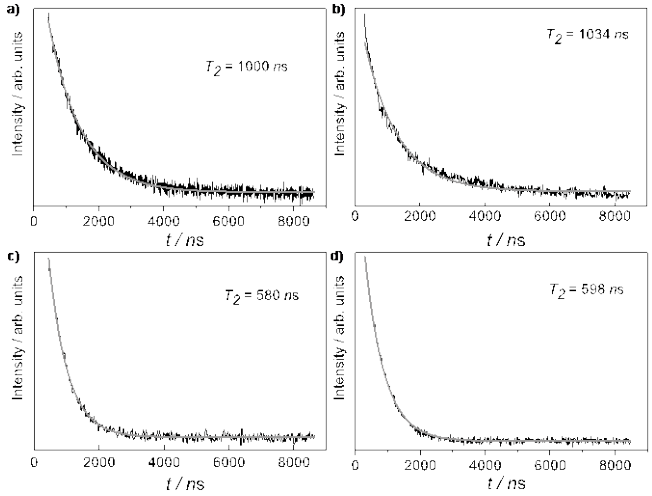

Figure S5. Phase memory times (T_m) for: compound **2** observed at (a) 314 mT (Cu transition) and (c) 409 mT ({Cr_7Ni} transition); compound **5** observed at (b) 305 mT (Cu transition) and (d) 387 mT ({Cr_7Ni} transition). A À/2-Ä-À-Äecho sequence was used with 64 ns pulses. The echo decays were fit to $Y(2Ä) = Y(Ä)\exp^{kTm}$.

Calculated dipolar interaction matrix for compound 2

The full dipolar matrix (in Hz) is calculated from:

$$\mathbf{D} = \frac{\mu_0 \mu_B^2}{4\pi h} \sum_{i=1}^{8} \frac{\mathbf{g}_{Cu} \cdot \mathbf{g}_i}{r_{i,Cu}^3} K_i \left(\mathbf{g}_{Cu} \cdot \mathbf{g}_i - 3(\mathbf{g}_{Cu} \cdot \mathbf{R})(\mathbf{R} \cdot \mathbf{g}_i) \right)$$

where μ_0, μ_B and h are the vacuum permittivity, the Bohr magneton and Planck's constant, respectively; i = 1–8 denotes the metal ion (M) positions in the {Cr_7Ni} ring; $\mathbf{g}_{Cu}$ and $\mathbf{g}_i$ are the **g**-matrices of the Cu(II) ion, Cr(III) or Ni(II) ions, $r_{i,Cu}$ are the Cu···M distances (average 8.56 Å); **R** is the unit vector parallel to Cu···M; and K_i are the projection factors for the i^{th} ion in {Cr_7Ni} onto the $S = {}^1/_2$ ground state (where £$_i$ K_i = 1). We have taken g_{Cr} and g_{Ni} as isotropic and 1.96 and 2.20, respectively. $\mathbf{g}_{Cu}$ is taken as axial with principal values $g_{\parallel}$ = 2.320 and $g_{\perp}$ = 2.055; the parallel direction is normal to the {Cr_7Ni} plane and makes a dihedral angle of 31° with the Cu···M vectors. The K_i values have been determined from paramagnetic NMR as 1.314, -1.126, 1.25, -1.126, 1.25, -1.126, 1.314 and -0.75 for i = 1 to 8, respectively, where position i = 8 is the Ni(II) ion. Note the projection of the g_i values above onto the $S = {}^1/_2$ ground state with these coefficients gives the experimentally observed g_{Cr7Ni} = £$_i$ $K_i g_i$ = 1.8.

With these values, and converting to units of cm^{-1}, we get:

$$\mathbf{D} = \begin{pmatrix} 0.0015 & 0.0003 & 0.0010 \\ 0.0003 & 0.0015 & -0.0010 \\ 0.0011 & -0.0011 & -0.0034 \end{pmatrix} \text{cm}^{-1}$$